Adatoms on Si(111) and Ge(111) surfaces

Robert D. Meade and David Vanderbilt

Lyman Laboratory of Physics, Harvard University, Cambridge, Massachusetts 02138

(Received 23 January 1989)

First-principles calculations of energy and stress are performed on adatom-covered Si(111) and Ge(111) surfaces. The presence of adatoms is found to lower the surface energy and cause a large change in surface stress. While the 1×1 surfaces are under a weak compressive stress, the $\sqrt{3} \times \sqrt{3}$ and 2×2 adatom-covered surfaces are under a strong tensile stress. Calculations at high plane-wave cutoff unambiguously identify the 2×2 top-site geometry as the energetically preferred adatom configuration. Relaxed geometries are presented and compared with x-ray structural measurements of adatoms in the Si(111)-7×7 structure. Vibrational mode frequencies and eigenvectors of the adatom unit are determined from a comprehensive set of frozen-phonon calculations for the Si 2×2 surface; we find two symmetric modes that are strongly localized at the surface, in agreement with electron-energy-loss–spectroscopy measurements. It is found that the 2×2 adatom-covered surfaces have three surface bands, and the dispersion relations are calculated along symmetry directions in the surface Brillouin zone. The surface band structures are in good agreement with angle-resolved photoelectron-spectroscopy data for the 7×7-Si(111) surface.

I. INTRODUCTION

Since the discovery that the annealed Si(111) surface reconstructs with a 7×7 surface cell,[1] a large amount of effort has been expended trying to understand this important surface. In the past several years, a variety of experimental techniques have been employed to study this 7×7 reconstruction,[2-6] and it is now widely accepted that the dimer–adatom–stacking-fault (DAS) model of Takanayagi *et al.*[2] correctly explains the atomic structure of annealed Si(111). In the Takanayagi model, triangular islands of faulted and unfaulted Si are separated by dimer walls. Within these islands, the surface is a simple adatom covering. The germanium surface, on the other hand, reconstructs with a $c2 \times 8$ surface cell. Recent structural studies have demonstrated[7-10] that this surface is a simple adatom covering, free of dimers and stacking faults. It is strange that germanium, which is chemically similar to silicon, reconstructs in such a different pattern.

What is the relation between these reconstructions? One common feature of the 7×7-Si(111) and $c2 \times 8$-Ge(111) reconstructions is that they both involve adatom coverings. There is a simple explanation why the presence of adatoms on a surface is energetically favorable. Consider an ideally terminated Si(111) surface with all the atoms in their ideal bulk positions, but with the crystal terminating at a (111) lattice plane. This 1×1 surface is never physically realized because it contains a high density of broken bonds, each of which is energetically costly. The density of these dangling bonds can be reduced by introducing "extra" atoms, called adatoms, onto the surface. Each adatom bonds to three surface atoms, but introduces only one new dangling bond. Thus, an adatom-covered surface will be energetically favorable because in covering the surface the density of broken bonds is reduced. There are two inequivalent

sites for the adatom, the top site, which is vertically over the atom in the second layer, and the hollow site, above the fourth-layer atom. Placing atoms in either site lowers the surface energy,[11] but the top site appears to be the only site observed experimentally.

Although each adatom reduces the dangling-bond density, it is not favorable to saturate a surface with adatoms. As we shall show, the 2×2 surface reconstruction, which accommodates only 75% of the original surface dangling bonds, is slightly lower in energy than the $\sqrt{3} \times \sqrt{3}$ structure, which accommodates all the dangling bonds. The simplest surfaces with one adatom for every four surface atoms (accommodating 75% of the broken bonds) have primitive unit cells with 4 times the area of the unreconstructed 1×1 surface. There are two such coverings, one with hexagonal symmetry, the 2×2 surface, and one with rectangular symmetry, the $c2 \times 4$ reconstruction. One can generate other coverings of this density, such as the $c2 \times 8$ observed on Ge, by decorating larger primitive cells; many of these are expected to be close in energy.[7,12] In this paper, we focus on the 2×2 adatom case with the hope that many features may be shared by similar surfaces. This is also the ordering observed locally within the islands of the DAS model.

Although the atomic structures of the 7×7 and $c2 \times 8$ surfaces have been established experimentally, it is still unclear why they are the energetically preferred reconstructions for Si and Ge respectively. Several authors have suggested that the relief of surface stress may be the driving force for the reconstruction of surfaces.[13-15] In this picture, the dimer walls function to relieve the compressive stress of the adatom-covered surface. However, preliminary calculations by Vanderbilt[16] indicated a strong *tensile* stress. An alternate model[17] suggests that the dimer walls are favored because they reduce the dangling-bond density. The role of surface stress has also been investigated experimentally. It has been found that

application of a lateral compressive stress to the Ge surface (by growth on Si) will drive it from a $c2 \times 8$ to a 7×7 reconstruction.[18] Similarly, application of compressive stress to the Si surface by alloying with Ge will drive the reconstruction from 7×7 to 5×5.[19] Thus there is strong evidence that surface stress plays an important role in determining the surface reconstruction.

In this paper a detailed discussion of the faulted and unfaulted adatom-covered surfaces of Si and Ge is presented, focusing on surfaces with a 2×2 periodicity with the adatoms in the top-site positions. Calculations of energy and stress for these surfaces have been performed, using first-principles self-consistent density-functional techniques. These highly converged, large-cell calculations were made possible by the use of an iterative diagonalization scheme developed recently.[20] [Some preliminary results on Si(111) surfaces have already appeared in Ref. 16, but these were limited to smaller cutoffs and thinner slabs.] The relaxed atomic coordinates of the adatom and subsurface Si atoms are presented and compared with the experimental positions determined by x-ray-diffraction studies.[21] The surface energies of the faulted and unfaulted adatom-covered surfaces of Si and Ge are investigated, including a discussion of the two sites for the adatom, the top and hollow positions. First-principles calculations of surface stress are presented, the results of which are in strong disagreement with those of semiempirical calculations by Pearson.[22] A good agreement is found between the calculated surface band structure and the angle-resolved photoemission spectra of the 7×7 surface.[23] The difference in band structure between the faulted and unfaulted surface is investigated, and the implications of these differences on the scanning tunneling microscopy images of the faulted and unfaulted halves of the 7×7 unit cell is discussed. Finally, surface-phonon frequencies have been determined via a set of frozen-phonon calculations, and the results compare well with electron-energy-loss–spectroscopy (EELS) measurements.

II. METHOD OF CALCULATION

Self-consistent density-functional calculations have been performed using the local-density approximation. We employed norm-conserving nonlocal pseudopotentials, which are optimally smooth, in accordance with the prescription of Vanderbilt.[24] The Hamiltonian was expanded in a basis of plane waves with a maximum energy of 8 Ry, with some tests carried up to 12 Ry. The dependence of energies and stresses on the plane-wave cutoff will be discussed later. The Hamiltonian was iteratively diagonalized using the method of Natarajan and Vanderbilt,[20] and the Hellmann-Feynman forces were determined. The bulk stresses were calculated as in Nielsen and Martin,[25] except that a correction due to finite basis size[26] was added.

Although one wishes to study the surface of a semi-infinite crystal, computationally one must choose a system with a finite cell. We used a slab five double layers (10 atoms) thick. For the 2×2 surfaces, the adatoms were then added to both the top and bottom surfaces, yielding a 42-atom cell with inversion symmetry through

the center of the slab. Periodicity normal to the surface was achieved by repeating the slabs with a spacing of eight double layers. This leaves approximately three double layers of vacuum between surfaces, which we found was enough space to prevent interaction across the vacuum. We fixed the lattice constant parallel to the surface to be that of the theoretical lattice constant at the working plane-wave cutoff. This is variationally correct for thick slabs, and is the best approximation for a thin slab modeling a semi-infinite surface. The Hamiltonian was diagonalized at representative k points in the irreducible Brillouin zone (IBZ). Specifically, the diagonalization was performed at seven k points in the IBZ of the 1×1 cell, four k points in the IBZ of the $\sqrt{3} \times \sqrt{3}$ cell, and three k points in the IBZ of the 2×2 cell. These k points were selected so that the seven-k-point set of the 1×1 IBZ and the four-k-point set of the $\sqrt{3} \times \sqrt{3}$ cell both project into the three-k-point set of the smaller 2×2 IBZ. Thus, the same subspace of the Hamiltonian was considered in all cases. The charge density at these k points was then used to generate a new potential,[27] using a calculated dielectric matrix as a guide.[28] This procedure was iterated until a self-consistent solution was found. Although the 1×1 geometry required a metallic filling, the adatom-covered 2×2 surface required only an insulating filling because of charge transfer in the unit cell. A simple insulating filling was used for the $\sqrt{3} \times \sqrt{3}$ adatom-covered surface. Having determined the electronic structure for this geometry, we calculated the Hellmann-Feyman forces on the atoms. We then moved the atoms in the unit cell to decrease these forces, using a calculated Keating force-constant matrix as a guide. This procedure was repeated until the forces were negligible (less than 0.02 eV/Å). The modified Broyden[29] convergence acceleration scheme was used to improve both the dielectric and Keating matrices as the calculations proceeded.

III. ATOMIC POSITIONS

We have calculated the relaxed geometry for several 2×2 adatom surfaces. The atomic positions of 2×2 adatom-covered unfaulted Si(111) are shown in Fig. 1, with the corresponding coordinates given in Table I. In Table I the coordinates are presented in the lattice vector basis $\mathbf{R} = c_1 \mathbf{A}_1 + c_2 \mathbf{A}_2 + c_z \mathbf{A}_z$, where $|\mathbf{A}_1| = |\mathbf{A}_2| = a_0/\sqrt{2}$ and $|\mathbf{A}_z| = a_0/\sqrt{3}$, and a_0 is the bulk lattice constant. By choosing $a_0 = 5.43$ Å we implicitly scale the positions to the experimental lattice constant. The actual calculations were performed at the theoretical lattice constant at 8 Ry, $a_0 = 5.47$ Å. We have not given the positions of all 42 atoms in the unit cell, but the missing coordinates can be related to those in Table I by symmetry. The coordinates of the atoms in the lower half of the slab may be generated by inversion symmetry through the slab center (the origin). The coordinates of the missing atoms (e.g., atoms 4 and 5) may be derived from those of the preceding on (e.g., atom 3) by 120° rotations through the $\hat{z}$-symmetry axis joining adatoms on the two surfaces of the slab. This has the effect of generating new components (c'_1, c'_2, c'_z) related to the old ones by
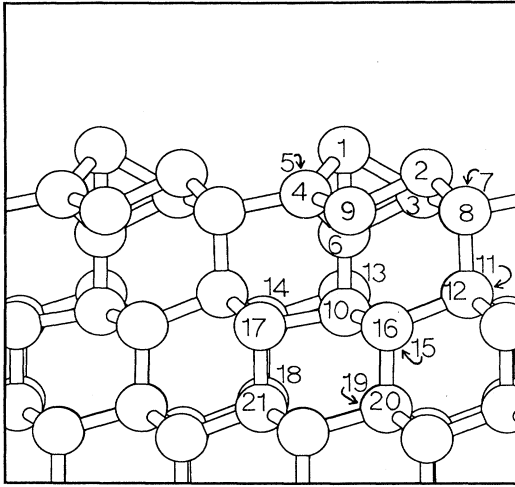
FIG. 1. A side view of the relaxed 2×2-adatom-covered Si(111) slab. The distance between adatoms is $\sqrt{2}a_0$. The corresponding atomic coordinates are presented in Table I.

$$(c_1',c_2',c_z')=(-c_2, c_1-c_2, c_z).$$

The Si(111) surface is a series of close-packed planes with a stacking sequence ($\cdots BCCAABBC$). Since the adatoms bond to surface atoms in the C positions, they may sit in either the B position (the top site) or in the A position (the hollow site). In Fig. 1 the adatom (atom 1) is in the top site. In a 2×2 reconstruction, there are four atoms in the top layer of the slab. The adatom bonds to three of these atoms, leaving one atom with a dangling bond, known as the rest atom (atom 2).

As can be seen in Fig. 1, the relaxed geometry of the adatom-covered surface involves many atoms being dis-

placed significantly from their ideal bulk positions. The nearest neighbors to the adatom (atoms 3–5) move closer together, and the second-layer atom beneath the adatom (atom 6) is displaced strongly downward. This, in turn, causes the third-layer atom beneath the adatom (atom 10) to be displaced downward, and the fourth-layer atoms to which it is bonded (atoms 15–17) to move outward. Although the $\hat{z}$ coordinate of any individual atom may change significantly from its bulk value, the average height of each layer remains close to the bulk height.

Although symmetry prohibits the rest atom from moving laterally, it does relax in the $\hat{z}$ direction. In its equilibrium position, the rest atom lies higher than the ideal bulk height by 0.3 Å. The rest atom has bond angles of 99.9° and bond lengths of 2.34 Å. This can be understood as a consequence of the charge transfer in the unit cell. While the surface band with most of its character on the adatom is unoccupied, the surface band composed of states localized on the rest atom is fully occupied (see Sec. VI). Thus the electronic structure of the negatively charged rest atom is similar to that of a neutral column-V element (e.g., As). As a consequence, the rest atom can be expected to relax upward in order to attain the p-like hybridization–it prefers, just as the As atom relaxes upward on the GaAs(110) surface. Alternatively, the upward relaxation can be regarded as being due to the electrostatic repulsion between the dangling-bond charge above the rest atom and the other three bond charges. In the hollow geometry, the occupied dangling-bond band has slightly less character on the rest atom, and the rest atom is slightly lower, with bond angles of 104.9° and bond lengths of 2.34 Å.

Also presented in Table I are the relaxed coordinates for the 2×2 adatom-covered surface with a plane-wave cutoff of 5 Ry. It is clear that the atomic positions are not greatly changed in going from 5 to 8 Ry. The largest

TABLE I. Relaxed atomic coordinates for 2×2 adatom-covered unfaulted Si(111). The positions are in lattice-vector coordinates, $\mathbf{R}=c_1\mathbf{A}_1+c_2\mathbf{A}_2+c_z\mathbf{A}_z$. $\mathbf{A}_1$ and $\mathbf{A}_2$ are the lattice vectors of the unreconstructed surface. They lie parallel to the surface, are separated by 120°, and have a length of $a_0/\sqrt{2}$, where a_0 is the bulk lattice constant. $\mathbf{A}_z$ points normal to the surface with a magnitude of one double layer, $a_0/\sqrt{3}$. Coordinates of unlisted atoms may be generated by symmetry (see text).

Atom no.	Calculated at 8 Ry			Calculated at 5 Ry			Bulk positions		
	c_1	c_2	c_z	c_1	c_2	c_z	c_1	c_2	c_z
1	0.000	0.000	2.497	0.000	0.000	2.493			
2	−0.667	0.667	2.279	−0.667	0.667	2.226	−0.667	0.667	2.125
3	0.317	0.634	2.084	0.316	0.633	2.092	0.333	0.667	2.125
6	0.000	0.000	1.720	0.000	0.000	1.728	0.000	0.000	1.875
7	−0.044	0.978	1.929	−0.030	0.985	1.924	0.000	1.000	1.875
10	0.000	0.000	0.996	0.000	0.000	1.005	0.000	0.000	1.125
11	−0.002	0.999	1.161	−0.001	0.999	1.157	0.000	1.000	1.125
14	0.667	−0.667	0.918	0.667	−0.667	0.912	0.667	−0.667	0.875
15	0.691	0.346	0.863	0.690	0.345	0.864	0.667	0.333	0.875
18	0.667	−0.667	0.168	0.667	−0.667	0.164	0.667	−0.667	0.125
19	0.680	0.340	0.110	0.678	0.339	0.111	0.667	0.333	0.125

change in bond length is from the adatom to its nearest neighbor, which is 2.47 Å in the 8-Ry calculation, but only 2.45 Å in the 5-Ry calculation.

Our calculated coordinates compare well with experimental measurements of lateral positions by x-ray diffraction. On the 2×2 surface neither the adatom nor the rest atom may relax its lateral coordinates, since both occupy positions of threefold symmetry. Atoms 3–5 relax inward (toward the adatom), but all three move by the same amount since they are constrained by symmetry. On the 7×7 surface the symmetry is lower. The adatoms on the islands are inequivalent and the nearest-neighbor bond lengths may vary. Robinson et al.[21] have performed x-ray-diffraction studies on the 7×7 Si(111) and have measured bond lengths projected into the (111) plane; the projected bond length between adatoms and surface atoms is found to vary from 2.07 to 2.13 Å, with an average value of 2.11 Å. This is closer to our calculated value of 2.106 Å than to the value of 2.072 Å calculated for the $\sqrt{3}\times\sqrt{3}$ adatom-covered surface.[30]

Although x-ray diffraction is a sensitive method of determining the lateral coordinates of surface atoms, it cannot determine their heights. However, Tong et al. have recently performed a sophisticated low-energy electron-diffraction (LEED) analysis to determine these heights. As in the previous case, we can compare calculated heights of the adatom-covered surface to the average heights on the 7×7 surface as determined by LEED. The majority of these heights are within the expected uncertainty of the LEED analysis, 0.1 Å. In the first bilayer, we find most coordinates to be in the range 0.03–0.11 Å higher than the LEED measurements, and find that this difference decreases to 0.04–0.05 Å in the second bilayer. Two notable exceptions are the rest atom, which we find ~0.5 Å higher than does Tong et al., and atom 6, which we find 0.2 Å higher. We also corroborate an interesting trend, which Tong et al. noted, concerning the difference in heights on the faulted and unfaulted surfaces. We find that the top bilayer on the faulted surface is an average of 0.036 Å higher than

the topmost bilayer of the unfaulted surface, close to the value of 0.05 Å resulting from the LEED analysis. This trend is also present in the 1×1 surface, for which the first bilayer of the faulted surface is higher than the first bilayer of the unfaulted surface by 0.09 Å (0.14 and 0.04 Å in the first and second layers, respectively). Chou, Cohen, and Louie[31] found a similar expansion for stacking faults in bulk systems, and also found relaxations of ~0.05 Å.

IV. ENERGIES

The surface energies we have calculated for several Si(111) and Ge(111) surfaces are presented in Table II. These results show that the adatom-covered surfaces are lower in energy than the 1×1 surfaces. Crudely, we can infer that the energy savings associated with decreasing the dangling-bond density offsets the energy cost of distorting the bond lengths and angles between the surface atoms. Moreover, we can conclude that of all the adatom-covered surfaces investigated, the 2×2 top-site covering had the lowest energy. This contradicts the naive expectation that the surface with the lowest density of dangling bonds will be the energetically favored one. Instead, we must consider the electronic structure of the surfaces. While the 2×2 top-site surface is an insulating filling of the favorable rest-atom band (see Sec. VI), the $\sqrt{3}\times\sqrt{3}$ top-site surface is a metallic filling of the adatom band. As an alternate explanation, one might guess that a higher adatom coverage might result in a lower degree of relaxation of the adatom cell. We have tested this by comparing the distance between adatom nearest neighbors (atoms 3–5 in Fig. 1) in different structures, a smaller distance indicates a greater relief of bond-angle stress. We found this distance to be 3.519, 3.590, and 3.648 Å in the $\sqrt{3}\times\sqrt{3}$, 2×2 hollow-site, and 2×2 top site, respectively (compared with a value of 3.839 Å for the bulk structure), and thus it appears differing degrees of structural relaxation are not responsible for the relative energies of the adatom surfaces. We also find that

TABLE II. Calculated surface energies and stresses for Si(111) and Ge(111) surfaces. All adatoms in top-site positions, except as noted. The structures were relaxed with an 8-Ry plane-wave cutoff, and the energies and stresses were calculated. The energies were then recalculated using a 12-Ry cutoff without further structural relaxation.

	Structure	E [eV/(1×1 cell)]		σ_{ii} [eV/(1×1 cell)]
		8 Ry	12 Ry	
Si	1×1	1.45	1.39	-0.54
	1×1 (faulted)	1.51		0.11
	$\sqrt{3}\times\sqrt{3}$-adatom	1.27	1.18	1.70
	2×2-adatom	1.24	1.12	1.66
	2×2-adatom (faulted)	1.27		1.89
	2×2-adatom (hollow site)	1.31	1.23	1.18
Ge	1×1	1.40		-0.73
	1×1 (faulted)	1.45		-0.26
	2×2-adatom	1.20		1.43
	2×2-adatom (faulted)	1.22		1.67

the introduction of a stacking fault into the top layer raises the surface energy slightly, in the range 0.02–0.06 eV/(1×1 cell). This is similar to the energy cost of a stacking fault in the bulk, which has been calculated to be ~0.04 eV/(1×1 cell).[31]

The pseudopotential calculations were performed on a slab geometry, and so we obtain the energy per slab unit cell, E_{slab}. The surface energy, E_{surf}, is related to the slab energy by

$$E_{surf} = E_{slab} - N_{atom}E_{bulk} ,\qquad (4.1)$$

where N_{atom} is the number of atoms in the slab unit cell, and E_{bulk} is the energy per atom of the bulk. In order to deduce E_{surf}, one must first obtain E_{slab} and E_{bulk}, which were calculated using three, four, or seven k points in the *slab* IBZ and 10 k points in the *bulk* IBZ, respectively. To test the impact of using different k-point sets to calculate the slab energies and bulk energies, we also calculated the Si bulk energy using a slablike geometry and k-point set. The slablike geometry had 6 atoms/(unit cell) and we employed the same k-point set as had been previously used for the surface calculations; we used seven k points in the surface IBZ and a dense set along the k_z direction. We found that changing the k-point set changed the value of E_{bulk} by 0.042 eV/(bulk unit cell). Although this lowered the absolute value of the surface

energies by ~0.12 eV/(1×1 cell), we found that the relative energies of different surfaces changed by at most 0.007 eV/(1×1 cell).

The relative energies of adatom-covered and adatom-free surfaces are found to have an unusually strong dependence on plane-wave cutoff, as can be seen in Fig. 2. At 5 Ry the π-bonded chain surface[32] is significantly lower in energy than the 2×2 adatom-covered surface, consistent with the results of Northrup.[11] If this were the case, it would be hard to understand why the 7×7 DAS surface should be lower in energy than the 2×1 π-bonded chain surface, since the former is only expected to be slightly more stable than the 2×2 adatom surfaces.[17] Fortunately, this is no longer the case at higher plane-wave cutoff. The energies of adatom-covered surfaces change significantly because the adatom cell contains a fivefold-coordinated site, with a complex bonding topology. Evidently, higher-energy plane waves are needed to correctly describe the electronic states of the adatom unit, which presumably involve significant d character.[33] On the other hand, the energies of the 1×1 and 2×1 surfaces remain relatively constant since the bonding on these surfaces is relatively simple. Note that the results at high plane-wave cutoff unambiguously identify the top-site 2×2 adatom surface as being significantly lower in energy than $\sqrt{3}\times\sqrt{3}$ or hollow-site competitors.

V. STRESSES

For each surface, we have also calculated the intrinsic surface stress, defined as

$$\sigma_{ij}^{surf} = \frac{1}{A}\frac{dE^{surf}}{d\epsilon_{ij}} ,\qquad (5.1)$$

where E^{surf} is the surface energy per unit cell, ϵ_{ij} is the surface strain tensor, and A is the equilibrium surface cell area. For an arbitrary surface, the only requirement on σ_{ij} is that it be symmetric. But, each of the surfaces we have considered is highly symmetric, containing a threefold-symmetry axis. This restricts the form of the surface stress tensor; it must be proportional to the identity matrix. The diagonal components of this matrix are presented in Table II. The results for Si and Ge are qualitatively similar. For both elements, the 1×1 ideal surface is under a small compressive stress (negative stress). When adatoms are introduced onto the surface, a relatively large tensile stress is induced. Finally, for both 1×1 and adatom-covered surfaces the presence of a stacking fault adds a small tensile stress.

We suggest the following interpretation of these results. The compressive stress in the 1×1 surfaces in introduced because the topmost atom has only one electron in its dangling bond. This atom could lower its energy by hybridizing with some sp^2 character, but cannot flatten because the perpendicular lattice constant is fixed. It does lie somewhat flatter than in the bulk, having a bond angle of 114° and bond lengths of 2.29 Å. The small tensile stress associated with the stacking fault may be understood by looking down the axis formed by atoms 6 and 10. In the ideal surface, the bond between atoms 6 and 3 and the bond between atoms 10 and 15 are stag-
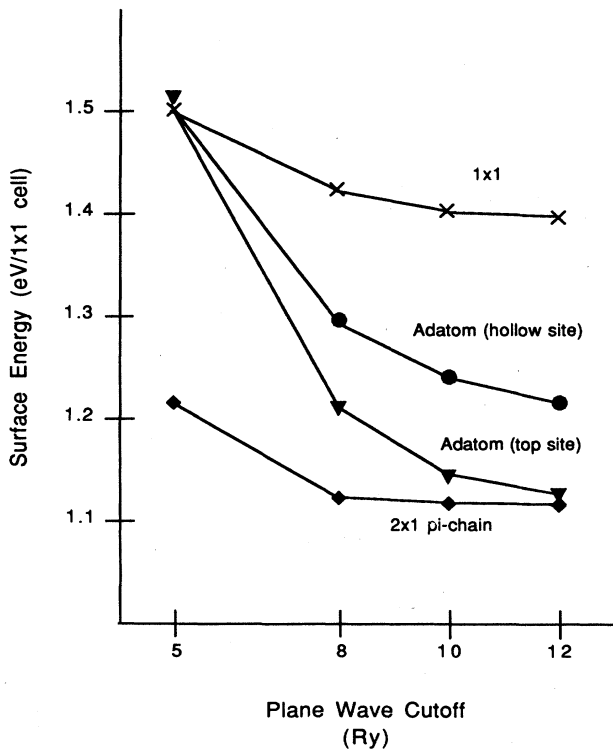

FIG. 2. The surface energies of several reconstructions as a function of plane-wave cutoff. The structures were relaxed with an 8-Ry cutoff, and the energies were calculated. The energies were then recalculated using 5-, 10-, and 12-Ry cutoffs without further structural relaxation.

gered. In the faulted surface these bonds are eclipsed, and this introduces a repulsive interaction due to the Pauli exclusion principle.[34] Hence, the topmost atom rises up (in the $\hat{z}$ direction), with angles of 112°, introducing a tensile stress.

Finally, the tensile stress of the adatom-covered surfaces is associated with the unnatural bonding topology of the adatom cell. The adatom and the second-layer atom beneath it (atom 6) are pushed apart, either by the Coulomb repulsion or by the energy gained from relieving the unnatural bond angle on the first-layer atoms. Although these atoms repel, they try to maintain their natural bond lengths with the atoms in the first layer. This causes a tensile stress and pulls the first-layer atoms closer together.

As with the energies, we have calculated the surface stresses at several plane-wave cutoffs. At a cutoff energy of 5 Ry, the stress of the 2×2 unfaulted adatom-covered Si(111) surface was 1.52 eV/(1×1 cell), slightly less than the stress calculated at a cutoff of 8 Ry. As in our discussion of energies, we expect that stress of the adatom-covered surfaces will be more sensitive to energy cutoff than surfaces with simpler bonding topologies. We also expect that the stress will vary less dramatically above 8 Ry than in the region up to 8 Ry.

VI. BAND STRUCTURE

The band structure of 2×2 adatom-covered Si was calculated along several symmetry directions, as shown in Fig. 3. This band structure includes several surface states. These states, whose energy lies in the gap, decay exponentially into the bulk. The top two surface bands, S_1 and S_2, are plotted against the projected band structure of the bulk calculations. As in many local-density-approximation (LDA) band structures, the bulk band gap is smaller than the experimental value, and we have not taken steps to correct this problem.[35] The energies of the different calculations were aligned by matching the potential in the bulk to the potential at the center of the slab. Also shown in Fig. 3 is the experimental surface band structure as determined by angle-resolved photoemission spectroscopy.[23] We have aligned the experimental band structure by requiring that the measured and calculated S_2 bands coincide. (It should be noted, however, that with this alignment, the valence-band maximum falls 0.35 eV lower than was indirectly inferred in Ref. 23.) Surprisingly, the theoretical separation between the two LDA surface bands is in good agreement with the experimental separation.

Of the two surface bands in Fig. 3, the lower band (S_2), which is fully occupied, has most of its character atop the rest atom (see Fig. 4). The upper band (S_1), which is unoccupied, has some of its character on the top of the adatom, and some in and below the adatom cell. This indicates that there is a charge transfer in the unit cell, from the adatom to the rest atom. There are two additional surface bands we have not shown in Fig. 4. They lie in the region -0.2 to -0.5 eV. (All energies are referred to the top of the valence band.) These two bands, which are nearly degenerate, are the backbonds from the
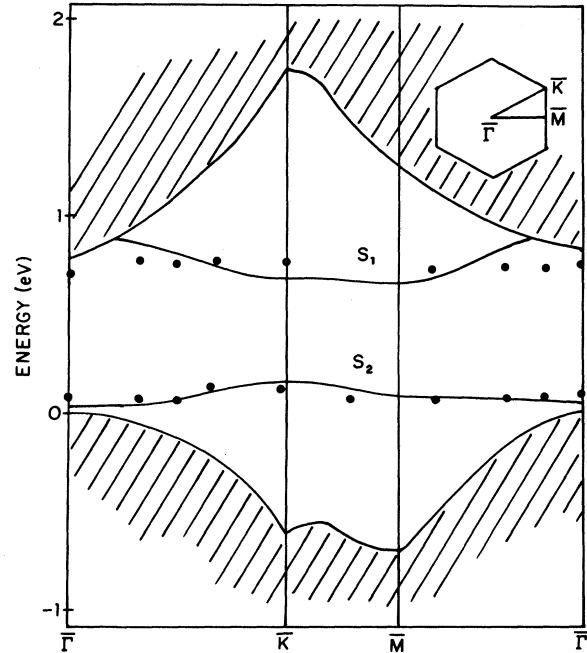

FIG. 3. The surface band structure of 2×2-adatom-covered Si(111) plotted in the 2×2 irreducible Brillouin zone. The curves S_1 and S_2 are the calculated dangling-bond bands whose charge densities are shown in Fig. 4. The shaded area is the bulk band structure projected onto the IBZ of the 2×2 surface cell. Dots represent the experimental angle-resolved photoemission spectroscopy data for the 7×7-Si(111) surface. The experimental points were aligned by requiring that the measured and calculated S_2 bands coincide.

adatom to the first-layer atoms.[11,23]

The charge density of these surface states, averaged over the IBZ, are shown in Fig. 4. The charge density of S_2 indicates that this is an sp^3-like band localized on the rest atom, with some small character on atoms in the second bilayer. The charge density of 4(b), however, indicates that the adatom states are not conventional dangling bonds. These states have significant character on the fivefold-coordinated atom (atom 6) and may be regarded as a band of floating bonds.[36] We have also generated charge-density plots (not shown) of the S_1 and S_2 bands of 2×2 adatom-covered Si(111) with the adatoms in the hollow site. As before, the S_2 band is a simple sp^3 hybrid band localized atop the rest atom. But now, because of the absence of the fivefold-coordinated site, the S_1 band has a more conventional dangling-bond character; it is localized primarily above the adatom, with some character below the adatom and very little character elsewhere.

The band structure has been calculated for both the faulted and unfaulted surfaces, and the top two surface states are shown in Fig. 5. As before, we align band structures from different calculations by matching the potentials at the center of the slabs. However, because of the finite thickness of the slab and the deep relaxations of the adatom cell, the potential in the middle of the slab
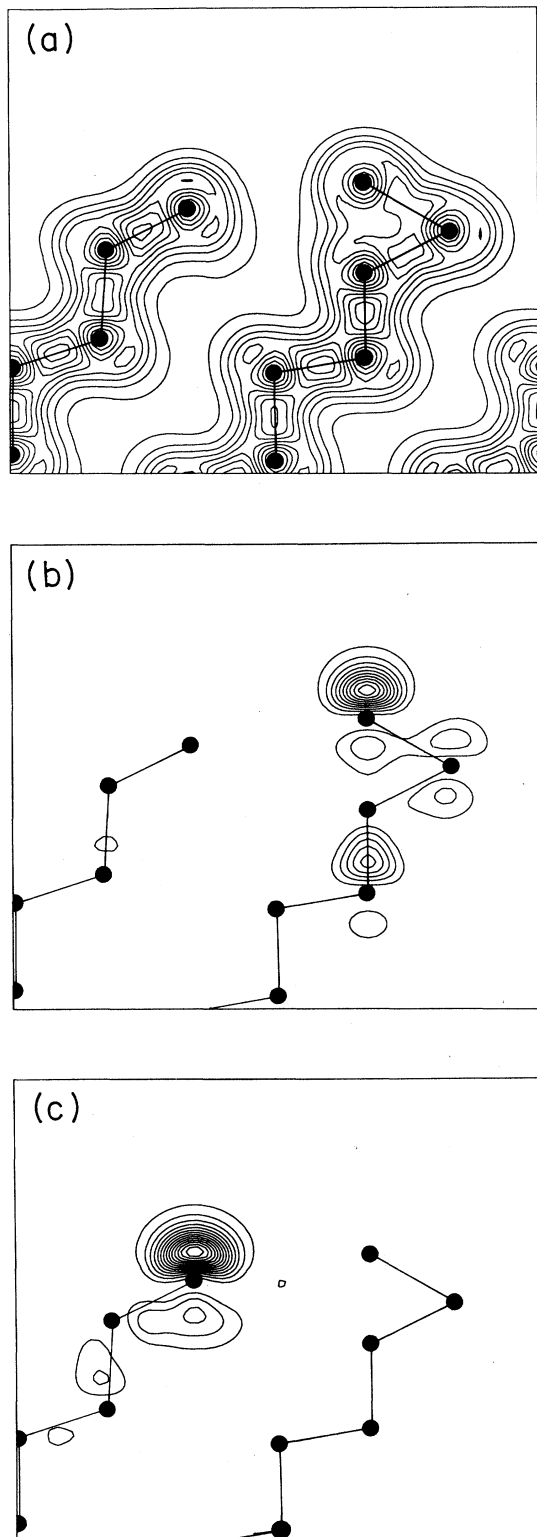
(a)

(b)

(c)

FIG. 4. Contour plots of the charge density of 2×2-adatom-covered Si(111). The figures show a cross section of the charge density on a plane passing through both the adatom and the rest atom. (a) is the total charge density. (b) and (c) show the average charge density of all states in bands S_1 and S_2, respectively.
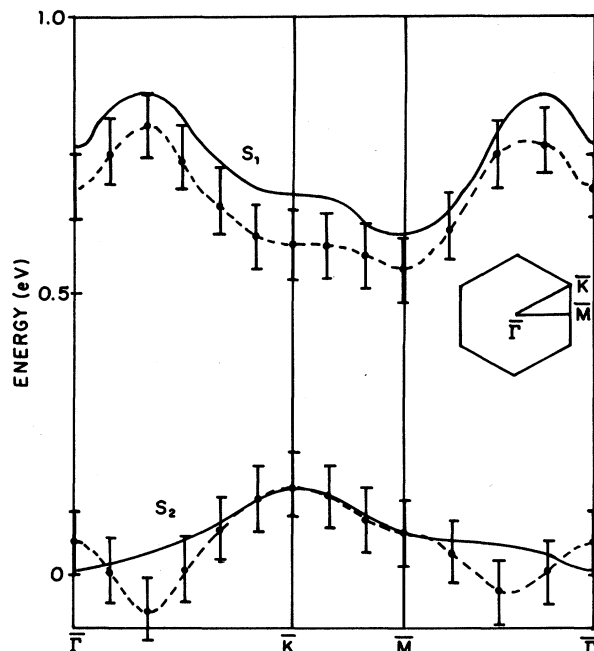

FIG. 5. The dangling bond bands of faulted and unfaulted 2×2-adatom-covered Si(111). The solid (dashed) bands correspond to the unfaulted (faulted) surface. The error bars result from ambiguities in aligning bands from different calculations.

differs slightly at inequivalent sites. For this reason, we have also employed an alternate method of aligning the bands, by aligning the bottom of the valence band (in which the states are primarily bulklike). The uncertainties in aligning bands from different calculations has been incorporated into the error bars in Fig. 4.

Although the results are somewhat ambiguous, it appears that the surface-state energies on the faulted surface are lower than on the unfaulted surface. If this is the case, then we expect a charge transfer on the 7×7 surface from the unfaulted to the faulted islands. This may explain the asymmetry between these islands seen in the low-bias-voltage STM images of the 7×7 surface in Refs. 3 and 5. It may also play some role in the asymmetric deposition of silver[37] and ammonia[38] on the 7×7 surface.

VII. ADATOM VIBRATIONS

We have also investigated the vibrational properties of the adatom unit. EELS experiments of Daum *et al.*[39] on the Si(111)-7×7 surface indicate a prominent loss feature at 570 cm^{-1} (above the top of the bulk-phonon continuum), and indications of a broader, weaker feature near 240 cm^{-1}. On the basis of cluster calculations, in which only two structural degrees of freedom were included, these features were assigned[39] to modes involving vertical motions of the adatom and its neighbor underneath (atoms 1 and 6 of Fig. 1), with out-of-phase and in-phase combinations giving rise to the high- and low-frequency modes, respectively. These assignments were subsequently supported and refined by calculations of the phonon

spectra for the full 7×7 surface using empirical potentials by Li et al.[40] These workers identified the same two prominent modes, but the high-frequency mode was found to have a significant weight on the third-layer atom beneath the adatom (our atom 10).

We have carried out LDA calculations of the adatom phonon modes on the unfaulted Si 2×2-adatom surface, making neither cluster nor empirical approximations. Because the EELS experiments are indicative of fully symmetric vibrations,[39] we have considered only distortions of our 42-atom unit cell that preserve all symmetries (including inversion through the center of the slab), and we restrict ourselves to phonons at the origin of the surface Brillouin zone (corresponding to displacements which preserve the 2×2 surface cell). This restricts us to 16 vibrational degrees of freedom or "basis modes," six of which correspond to vertical motions of atoms lying on threefold-symmetry axes, and 10 of which correspond to coherent vertical or breathing motions of triplets of atoms related to one another by threefold rotations.

We have calculated the full 16×16 dynamical matrix describing these symmetric vibrational degrees of freedom. Each column of the dynamical matrix was determined by calculating the forces on all the atoms for displacements of 0.04 Å of the corresponding basis-mode coordinate, and then projecting the forces onto each of the basis modes to obtain the appropriate elements of the dynamical matrix. (Actually, differences were obtained using displacements of ±0.04 Å in order to eliminate errors due to cubic anharmonic terms in the crystal energy.) The matrix was then diagonalized, yielding the eigenvectors and eigenvalues for the 16 symmetric normal modes of the system.

Of these, only two were found to be strongly localized near the surface (having 75% of their character in the top double layer plus adatom). These have frequencies of 267 and 532 cm^{-1} and eigenvectors illustrated in Figs. 6(a) and 6(b), and thus we identify them with the broad low-frequency and sharp high-frequency features in the EELS spectrum respectively.[39] The nature of these normal modes is qualitatively similar to the results based on two degrees of freedom reported by Daum et al.,[39] and in close agreement with the results of Li et al.[40] Like the latter, we find that the low-frequency mode involves substantial motion of atoms 3 and 10, while the high-frequency mode has a larger amplitude on atom 10 than on the adatom. The calculated frequency of the high-frequency mode is 7% lower than experiment; most likely the difference between the adatom environment on a 2×2-adatom surface (theory) and on the 7×7 surface (experiment), particularly the larger stress expected for the latter case,[16] is responsible for this discrepancy.
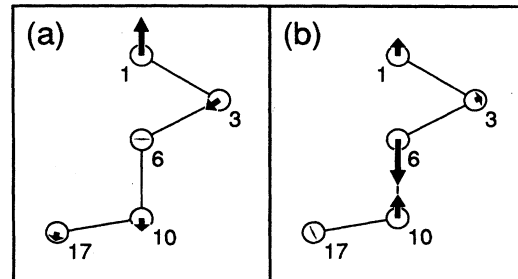

FIG. 6. Phonon-normal-mode displacements for the symmetric adatom vibrations at (a) 267 cm^{-1} and (b) 532 cm^{-1}. The orientation of the figure is identical to that of Fig. 4.

We also find that the high-frequency mode is more highly localized than the low-frequency feature in the lateral as well as vertical directions, having less than 1% of its character on atoms other than those shown in Fig. 6(b) and their symmetry-related partners. Thus we expect this state to have very little dispersion in the surface Brillouin zone compared to the low-frequency mode. This is in qualitative agreement with the widths of the features observed experimentally.

VIII. SUMMARY

We have performed *ab initio* calculations of several 2×2 adatom-covered surfaces. We have calculated relaxed geometries, surface energies and stresses, surface band structures, and surface-phonon frequencies. The Si(111) 2×2-adatom positions agree well with the surface x-ray studies by Robinson et al.[21] We found that the surface stress was tensile, which is inconsistent with the stress-relief model of DAS formation. The calculated surface band structure was found to agree well with the experimental measurements of Uhrberg et al.[23] Finally, the frequencies and mode eigenvectors of symmetric surface-phonon modes were determined, and found to be consistent with EELS measurements of Daum et al.[39]

ACKNOWLEDGMENTS

[1] R. E. Schlier and H. E. Farnsworth, J. Chem. Phys. **30**, 917 (1959).

[2] K. Takayanagi, Y. Tanishiro, M. Takahashi, and S. Takahashi, J. Vac. Sci. Technol. A **3**, 1502 (1985); Surf. Sci. **164**, 367 (1985).

[3] R. S. Becker, J. A. Golovchenko, E. G. McRae, and B. S. Swartzentruber, Phys. Rev. Lett. **55**, 2028 (1985).

[4] R. M. Tromp and E. J. van Loenen, Surf. Sci. **155**, 441 (1985).

[5] R. J. Hamers, R. M. Tromp, and J. E. Demuth, Phys. Rev. Lett. **56**, 1972 (1986).

[6]H. Huang, S. Y. Tong, W. E. Packard, and M. B. Webb, Phys. Lett. A **130**, 166 (1988); S. Y. Tong, H. Huang, C. M. Wei, W. E. Packard, F. K. Men, G. Glander, and M. B. Webb, J. Vac. Sci. Technol. A **6**, 615 (1988).

[7]R. S. Becker, J. A. Golovchenko, and B. S. Swartzentruber, Phys. Rev. Lett. **54**, 2678 (1985).

[8]W. E. Packard and M. B. Webb, Surf. Sci. **195**, 371 (1988).

[9]R. Feidenhans'l, J. S. Pedersen, J. Bohr, M. Nielsen, F. Grey, and R. L. Johnson, Phys. Rev. B **38**, 9715 (1988).

[10]P. M. J. Marée, K. Nakagawa, J. F. van der Veen, and R. M. Tromp, Phys. Rev. B **38**, 1585 (1988).

[11]J. E. Northrup, in *Proceedings of the Eighteenth International Conference on the Physics of Semiconductors,* edited by O. Engström (World Scientific, Singapore, 1987), p. 61.

[12]D. Vanderbilt, in *The Structure of Surfaces II,* edited by J. F. van der Veen and M. A. Van Hove (Springer-Verlag, New York, 1988), p. 276.

[13]J. C. Phillips, Phys. Rev. Lett. **45**, 905 (1980).

[14]E. G. McRae, Phys. Rev. B **28**, 2305 (1983); Surf. Sci. **147**, 663 (1984); **163**, L766 (1985).

[15]T. Ichikawa and S. Ino, Surf. Sci. **136**, 267 (1984).

[16]D. Vanderbilt, Phys. Rev. Lett. **59**, 1456 (1987).

[17]D. Vanderbilt, Phys. Rev. B **36**, 6209 (1987).

[18]H. J. Gossman, J. C. Bean, L. C. Feldman, D. G. McRae, and I. K. Robinson, Phys. Rev. Lett. **55**, 1106 (1985).

[19]K. Nakagawa, P. M. J. Maree, J. F. van der Veen, and R. M. Tromp, in *Proceedings of the Eighteenth International Conference on the Physics of Semiconductors,* edited by O. Engström (World Scientific, Singapore, 1987), p. 93.

[20]R. Natarajan and D. Vanderbilt, J. Comput. Phys. **81**, 218 (1989).

[21]I. K. Robinson, W. K. Waskiewicz, P. H. Fuoss, and L. J. Norton, Phys. Rev. B **37**, 4325 (1988).

[22]E. Pearson, T. Takai, T. Halicioglu, and W. A. Tiller, J. Cryst. Growth **70**, 33 (1984).

[23]R. I. Uhrberg, G. V. Hansson, J. M. Nicholls, and P. E. S. Persson, Phys. Rev. B **31**, 3805 (1985).

[24]D. Vanderbilt, Phys. Rev. B **32**, 8412 (1985).

[25]O. H. Nielsen and R. M. Martin, Phys. Rev. B **32**, 3792 (1985).

[26]R. D. Meade and D. Vanderbilt, in *Atomic Scale Calculations in Materials Science,* Vol. 141 of *Materials Research Society Symposium Proceedings,* edited by J. Tersoff, D. Vanderbilt, and V. Vitek (MRS, Pittsburgh, 1989), p. 451.

[27]E. P. Wigner, Phys. Rev. **36**, 1002 (1934).

[28]K. M. Ho, J. Ihm, and J. D. Joannopoulos, Phys. Rev. B **25**, 4260 (1982).

[29]D. Vanderbilt and S. G. Louie, Phys. Rev. B **30**, 6118 (1984).

[30]J. E. Northrup, Phys. Rev. Lett. **57**, 154 (1986).

[31]M. Y. Chou, M. L. Cohen, and S. G. Louie, Phys. Rev. B **32**, 7979 (1985).

[32]K. C. Pandey, Phys. Rev. Lett. **47**, 1913 (1981); **49**, 223 (1985).

[33]G. X. Qian and D. J. Chadi, Phys. Rev. B **35**, 1288 (1987).

[34]E. B. Wilson, Jr., Adv. Chem. Phys. **2**, 367 (1959); J. P. Lowe, J. Chem. Phys. **45**, 3059 (1966).

[35]M. S. Hybertsen and S. G. Louie, Phys. Rev. B **34**, 5390 (1986).

[36]S. Pantelides, Phys. Rev. Lett. **58**, 1344 (1987).

[37]St. Tosch and H. Neddermeyer, Phys. Rev. Lett. **61**, 349 (1988).

[38]R. Wolkow and Ph. Avouris, Phys. Rev. Lett. **60**, 1049 (1988).

[39]W. Daum, H. Ibach, and J. E. Müller, Phys. Rev. Lett. **59**, 1593 (1987).

[40]X.-P. Li, G. Chen, P. B. Allen, and J. Q. Broughton, Phys. Rev. B **38**, 3331 (1988).